

Supporting Information

Kernel-Based Microfluidic Constriction Assay for Tumor Sample Identification

Xiang Ren[†], Parham Ghassemi[†], Yasmine M. Kanaan^{‡1}, Tammey Naab^{‡2}, Robert L. Copeland^{‡3}, Robert L. Dewitty[§], Inyoung Kim[⊥], Jeannine S. Strobl[†], Masoud Agah^{†*}

[†] The Bradley Department of Electrical and Computer Engineering, Virginia Tech, Blacksburg, VA, 24061

[‡] Howard University, College of Medicine, Cancer Center, ¹Microbiology Department, ²Pathology Department, ³Pharmacology Department, Washington, DC, 20059

[§] Howard University Hospital, Providence Hospital, Washington, DC, 20017

[⊥] Department of Statistics, Virginia Tech, Blacksburg, VA, 24061

Table of Contents

1	Materials and methods: Human subjects and clinical data	S-2
2	Materials and methods: Patient sample preparation and post-experiment collection.....	S-3
3	Fabrication processes.....	S-4
4	Breast Cell lines video/image	S-5
5	Verification of the identity of cells as cancer versus non-tumorigenic (MCF-10A) at the single cell level.....	S-6
6	Full table of prediction values	S-7

1 Materials and methods: Human subjects and clinical data

Tissue specimen A was collected from an African American (AA) woman who was diagnosed with breast cancer (BCa) at age 58 and received chemotherapy and radiation therapy before surgery; invasive ductal carcinoma (IDC); Grade 3; metastatic dimension 4.5 cm; nuclear grade 2/3; ER-positive (>95%), PR-positive (>35%), Her2-negative (+1); 5/8 positive lymph nodes for metastatic carcinoma; glandular tubular differentiation (Score 3); mitotic score (score 2); nuclear pleomorphism 3; Grade 3; Stage upT2, pM2a, ER-positive (99.9%), PR-positive (17.8%); HER2-positive (2+).

Tissue specimen B was collected from 73 years old AA female; diagnosed with TNBC [ER-negative (0.0%), PR-negative (0.0%), Her2-negative (+1)]; IDC; Grade 3 with focal necrosis; no evidence of metastatic carcinoma in lymph nodes (0/5); immunohistochemical studies show the tumor cells staining for cytokeratin 5/6; and personal history of lung cancer.

Tissue collection:

Breast cancer tumor and adjacent normal tissue were obtained from the same patient who was undergoing total or partial mastectomy. Briefly, fresh breast tissue samples were collected immediately after surgical resection in sterile culture medium [500 mL Dulbecco modified Eagle's medium (DMEM), 50 mL fetal bovine serum (FBS), 20 mL penicillin/streptomycin (100×), 2 mL Gentamicin (10 mg/mL), 1 mL Fungizone (250 µg/mL), 1 mL Nystain (50 mg/mL); Reagents from Stemcell Technologies, Vancouver, British Columbia].

Dissociation of human mammary tissue:

The tissue specimens were minced with a sterile scalpel into approximately 1 mm small fragments and collected in sterile tubes containing 9 mL of DMEM/12 medium supplemented with 2% FBS (Stemcell Technologies, Vancouver, British Columbia), 1 mL of 10× collagenase/Hyaluronidase (Stemcell Technologies, Vancouver, British Columbia), and the minced tissues were gently dissociated on a rotary shaker at 37°C for approximately 16 hours until complete disaggregation of fragments were obtained. After dissociation, the cell suspension centrifuged at 80× g for 30 seconds with the brake on, discard the liquefied fat layer and the supernatant was transferred to 50 mL tubes. The remaining cell "pellet 1" is highly enriched in epithelial organoids. The supernatant was centrifuged at 200× g for 3 minutes. The cell "pellet 2" from this second centrifugation contains variable numbers of epithelial, stromal and red blood cells. The supernatant from the second centrifugation, is a single cell suspension enriched for human mammary fibroblast, was centrifuged at 350× g for 5 minutes and the fibroblast cell "pellet 3" was cryopreserved in Complete EpiCult™-B Medium (Stemcell Technologies) supplemented with 50% FBS (Stemcell Technologies, Vancouver, British Columbia) and 6% Dimethyl Sulfoxide (DMSO) and stored in liquid nitrogen for future studies.

Generation of single-cell suspensions from dissociated human mammary tissue:

Briefly, the isolated pellets "1 and 2" were re-suspended in 1-5 mL of pre-warmed Trypsin-EDTA (0.25%), and 10 mL of cold HF solution [Hanks' Balanced Salt Solution (HBSS) Modified with 10 mM HEPES and supplemented with 2% FBS] was added. Centrifuging at 350× g for 5 minutes, and the pellet were re-suspended with 2 mL of pre-warmed 5mg/mL Dispase (Stemcell Technologies) and 200ul of 1mg/mL deoxyribonuclease 1 (DNase I) (Stemcell Technologies). The cell suspension was further diluted with an additional 10 mL of cold HF and filtered through a 40 µm cell strainer (Stemcell Technologies), and centrifuged at 350× g for 5 minutes. If the cell pellets were heavily contaminated with red blood cells, the pellets were re-suspended in a 1:4 mixture of cold HF [Hanks' Balance Salt Solution (HBSS) with 10 mM HEPES, 2% FBS]: Ammonium chloride solution and centrifuged at 450× g for 5 minutes. The cell viability was determined by the trypan blue exclusion technique (viability was 60% to 75%). The cells were cryopreserved into sterile cryo-tubes in 1.5 mL freezing medium [Complete EpiCult™-B Medium (Stemcell Technologies), 50% FBS (Stemcell Technologie), 6% DMSO] and stored in liquid nitrogen for further studies.

2 Materials and methods: Patient sample preparation and post-experiment collection

Hematoxylin and Eosin (H&E) Immunohistochemistry (IHC) Staining:

The cells were fixed with Thermo Scientific™ Richard-Allan Scientific™ Fix-Rite™ 2 (Thermo Scientific) and H&E staining performed with the standard procedure.

Immunohistochemical staining for CD45, CD68, and pancytokeratin was performed on a the automated Leica Bond™ system in combination with Bond Polymer Refine Detection, using standard protocol. All antibodies were purchased from Leica Biosystems.

The pancytokeratin or multi-cytokeratin is composed of the clones AE1 and AE3, which are specific for the 56.5, 50, 50', 48 and 40 kD acidic cytokeratins as well as the 65 to 67, 64, 59, 58, 56 and 52 kD basic cytokeratins. The cocktail of clones AE1 and AE3 exhibit broad reactivity with two families of cytokeratin, acidic and basic. Clones AE1/AE3 stain the cytoplasm of epithelial cells in the breast. Multi-Cytokeratin (AE1/AE3) is recommended for the characterization of normal and malignant epithelial cells. Enzyme pretreatment for AE1/AE3 uses the Bond proteolytic Enzyme 1 for 10 minutes at 37°C.

The CD45 antigen (leukocyte common antigen) is a family of five high molecular weight glycoproteins present on the surface of the majority of the human leukocytes (including lymphocytes, monocytes and eosinophils) but absent from erythrocytes and platelets. Clone X16/99 detects the CD45 antigen (leucocyte common antigen) on the membrane of leukocytes, including lymphocytes, macrophages and granulocytes. Pretreatment for CD45 is heat induced epitope retrieval at low pH using the Bond Epitope Retrieval Solution 1 for 20 minutes.

The CD68 molecule is a 110 kD intracellular glycoprotein primarily associated with cytoplasmic granules and to a lesser extent the membranes of macrophages. Markers to CD68 antigen are the most frequently used for the identification of macrophages in immunohistochemistry. Pretreatment for CD68 is heat induced epitope retrieval at high pH using the Bond Epitope Retrieval Solution 2 for 20 minutes.

Antibody detection used an HRP conjugated compact polymer system. DAB was used as the chromogen. The section was then counterstained with haematoxylin.

For multi-cytokeratin, strong cytoplasmic staining of malignant tumor cells is interpreted as positive.

For CD45, strong membrane staining of leukocytes is interpreted as positive.

For CD68, strong staining of the cytoplasm and the cell membrane of a monocytes, macrophages, and granulocytes is interpreted as positive.

3 Fabrication processes

The microchannel was molded with two layer SU-8 for PDMS soft-lithography, which requires a good strength and adhesion. Therefore, we used SU-8 3005 (MicroChem, Newton, MA) on a clean and dehydrated silicon prime wafer. Compared to SU-8 2000 series, SU-8 3000 series have an increased adhesion strength of 69 mPa, where SU-8 2000 series have only 38 mPa. The first layer SU-8 3005 was spin coated at 2000 rpm with an acceleration of 400 r/s for 30 s. This SU-8 layer was ~ 8 μm in thickness. Then, the wafer was soft baked at 65°C for 10 min and followed by 95°C for 35 min. After the wafer with uncured SU-8 was cooled down to room temperature, the wafer was moved to a mask aligner (Karl Suss MA-6, SUSS MicroTech, Inc., Corona, CA) and covered with a negative photo mask with patterned cavity and channel structures. The exposure time was set to 40.7 s at 8.6 mW/cm², which provided a total dose of 350 mJ/cm² of i-line (365 nm) UV on the wafer. After the first UV exposure, the wafer was transferred to a hot plate for post exposure bake at 65°C for 10 min and followed by 95°C for 30 min. After the wafer cooled down to room temperature after the post bake, the wafer was immersed in SU-8 developer (MicroChem, Newton, MA) for 5 min to remove the uncured SU-8. The wafer with the first layer SU-8 pattern with the constriction channel structures was cleaned by isopropanol and DI water, then dried with a nitrogen gun.

Tridecafluoro-1,1,2,2-tetrahydrooctyl-1-trichlorosilane (TFOCS, Fisher Scientific) was coated on the surface of the molds for the easy release of PDMS. 0.3 mL of TFOCS was dropped on the surface of a petri-dish, with the mold placed next to the droplets. Then, the petri-dish was moved into a vacuum chamber for 30 min. The TFOCS fully evaporated and formed a Teflon-like surface on the SU-8 mold. After the mold was prepared, standard PDMS replica molding was conducted to fabricate microchannel.

PDMS pre-polymer (SYLGARD® 184 silicone elastomer, Dow Corning, Midland, MI) and curing agent (SYLGARD® 184 silicone elastomer curing agent, Dow Corning, Midland, MI) mixture with a weight ratio of 10:1 was poured on the silicon with the SU-8 mold. The mixture was then placed in a vacuum container for 30 min to remove all the air bubbles. The degassed PDMS mixture was poured onto the mold and placed in a 65°C oven for 24 hours for the solidification of PDMS. The PDMS channels were then bonded to a glass slide after air plasma treatment using plasma cleaner (Harrick Plasma, model PDC-001, Ithaca, NY).

4 Breast Cell lines video/image

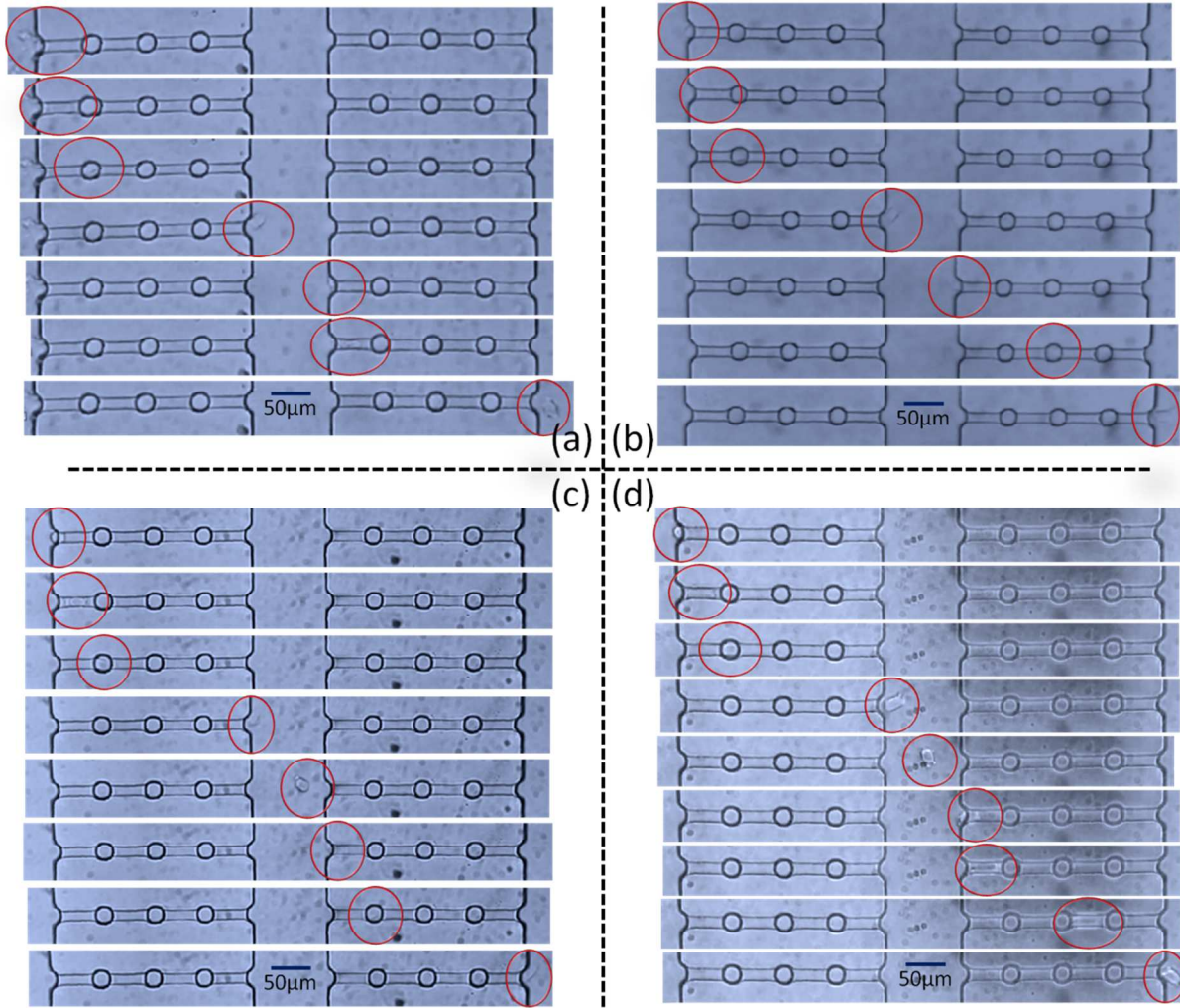


Figure S1. Breast cell line image from high speed video: (a) MDA-MB-231; (b) HCC-1806; (c) MCF-7; (d) MCF-10A.

The cancer cell line MDA-MB-231 deformed faster at the segment ① of SDC1. After passing through SDC1, the MDA-MB-231 cells were recovered back to spherical geometry before deforming at the entrance (segment ⑨) of SDC2. The normal cell line MCF-10A cells experienced a different passing procedure. MCF-10A cells have a higher stiffness when compared to that of cancer cells. This can translate in a longer deformation time at the segment ① of SDC1. After passing through SDC1, the MCF-10A cells were not fully recovered back to the spherical shape. This resulted in a longer time to deform and get into the entrance of SDC2 (segment ⑨). Once the MCF-10A cells started to pass through SDC2, the cells reduced the velocity in passing through the constriction regions in SDC2 due to maintaining their deformed rod shape.

Video file: video.avi.

5 Verification of the identity of cells as cancer versus non-tumorigenic (MCF-10A) at the single cell level

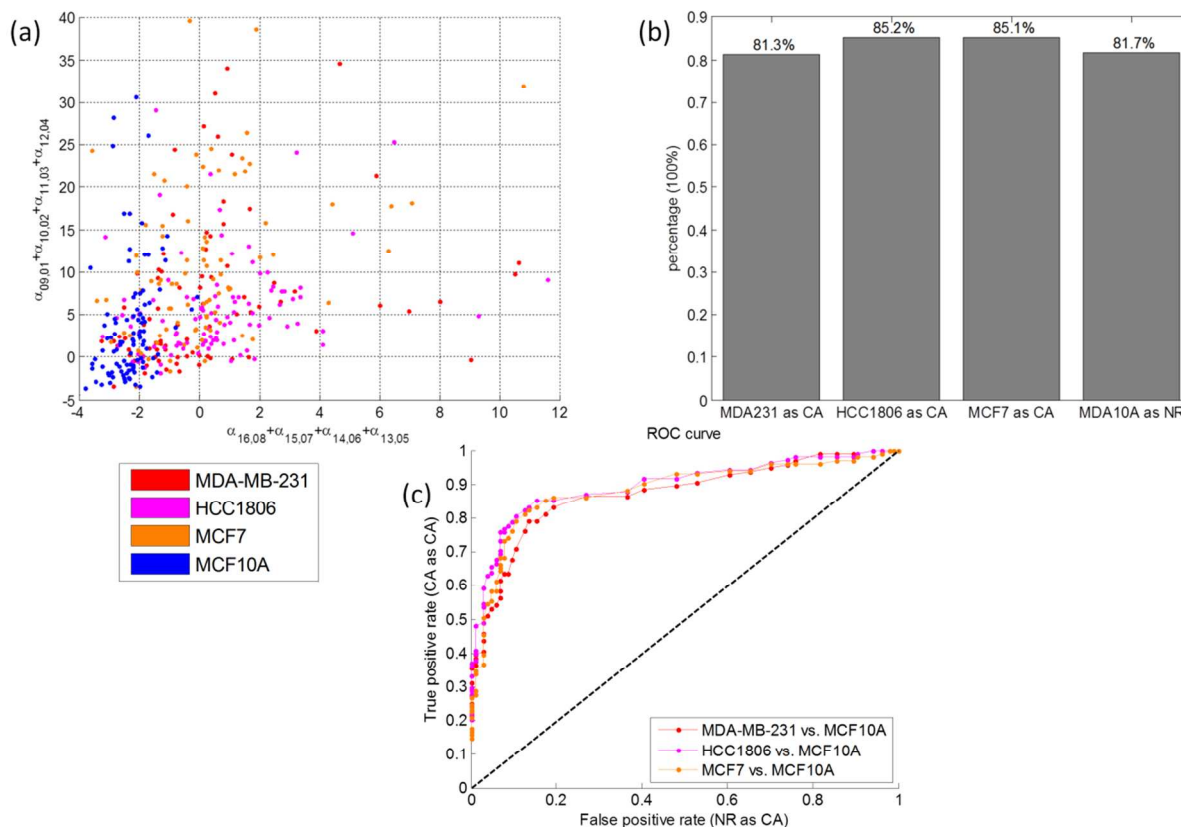


Figure S2. (a) Scattered plot of velocity increments of cell lines MDA-MB-231 (red), HCC-1806 (pink), MCF-7 (orange), and MCF-10A (blue); (b) prediction rate of distinguishing cancer cell lines as cancer, and MCF10A (non-tumorigenic) cells as normal; (c) receiver operating characteristic (ROC) curve of the prediction values between cancer cell lines and normal cell lines.

In Figure S2a, each dot represents one cell's velocity data using the variables selected from NGK model. The scatter plot of the velocity increments of the cell lines demonstrated a separation between cancer cell lines and normal cell line. The velocity increments parameters were selected based on the large population data analysis study by NGK model. We established a threshold to distinguish cancer cells from normal cells using the selected variables. From the scatter plot, we defined a threshold line to distinguish cancer cells from normal cells using:

$$\alpha_{16,08} + \alpha_{15,07} + \alpha_{14,06} + \alpha_{13,05} < Th$$

where the Th was a threshold for velocity increments. The receiver operating characteristic (ROC) curve in Figure S2c showed the trends of probability of distinguishing cancer cells from normal cells. The upper left corner data in Figure S2c indicated that a true positive rate of 80-85% was the ideal threshold for distinguishing cancer cells from MCF-10A, where the threshold $Th = -1.8$. Then, we applied the criteria:

$$\begin{cases} \text{CA: } \alpha_{16,08} + \alpha_{15,07} + \alpha_{14,06} + \alpha_{13,05} > -1.8 \\ \text{NR: } \alpha_{16,08} + \alpha_{15,07} + \alpha_{14,06} + \alpha_{13,05} < -1.8 \end{cases}$$

As shown in Figure S2b, we have the prediction rate of identifying MDA-MB-231, HCC-1806 and MCF-7 as cancer cells at 81.3%, 85.2% and 85.1%, respectively. The prediction rate of recognizing MCF-10A as normal cells at 81.7%.

6 Full table of prediction values

Table S1. Prediction values of cells using three methods: Ridge, NGK, and Lasso, respectively.

Cell names and Methods		Prediction Values (100%)					
		min	Q25	Q50	Q75	max	mean
MDA-MB-231 vs. MCF-10A	Ridge	0.8100	0.8100	0.8150	0.8200	0.8200	0.8155
	NGK	0.8200	0.8250	0.8350	0.8400	0.8450	0.8335
	Lasso	0.8300	0.8350	0.8400	0.845	0.8450	0.8385
HCC-1806 vs. MCF-10A	Ridge	0.8255	0.8302	0.8302	0.8349	0.8396	0.8316
	NGK	0.8208	0.8349	0.8396	0.8443	0.8491	0.8387
	Lasso	0.8160	0.8160	0.8184	0.8255	0.8349	0.8212
MCF-7 vs. MCF-10A	Ridge	0.8049	0.8098	0.8122	0.8195	0.8293	0.8137
	NGK	0.7951	0.8000	0.8049	0.8049	0.8098	0.8029
	Lasso	0.8195	0.8293	0.8317	0.8439	0.8439	0.8337
(MDA-MB-231 & HCC-1806 & MCF-7) vs. MCF-10A	Ridge	0.7971	0.8093	0.8117	0.8142	0.8142	0.8100
	NGK	0.7848	0.7922	0.7958	0.8020	0.8068	0.7961
	Lasso	0.8166	0.8191	0.8191	0.8215	0.8240	0.8198
MDA-MB-231 vs. HCC-1806	Ridge	0.6814	0.6912	0.7059	0.7206	0.7255	0.7049
	NGK	0.6667	0.6765	0.6863	0.6912	0.6961	0.6838
	Lasso	0.6716	0.6765	0.6814	0.6912	0.7059	0.6833
MDA-MB-231 vs. MCF-7	Ridge	0.6345	0.6497	0.6548	0.6548	0.6802	0.6538
	NGK	0.6294	0.6345	0.6421	0.6599	0.6802	0.6482
	Lasso	0.6091	0.6193	0.6269	0.6447	0.6599	0.6305
HCC-1806 vs. MCF-7	Ridge	0.7033	0.7177	0.7297	0.7368	0.7368	0.7263
	NGK	0.7464	0.7608	0.7632	0.7703	0.7751	0.7636
	Lasso	0.7560	0.7703	0.7799	0.7847	0.7847	0.7766
Patient A's CA vs. Patient A's NR	Ridge	0.7212	0.7308	0.7308	0.7404	0.7500	0.7337
	NGK	0.7212	0.7500	0.7596	0.7788	0.7885	0.7596
	Lasso	0.7692	0.7788	0.7885	0.7885	0.7981	0.7846
Patient B's CA vs. Patient B's NR	Ridge	0.6395	0.6463	0.6599	0.6667	0.6871	0.6592
	NGK	0.6735	0.6803	0.7007	0.7075	0.7143	0.6959
	Lasso	0.6871	0.6939	0.6973	0.7143	0.7279	0.7034
Patient A's CA vs. Patient B's CA	Ridge	0.5682	0.5739	0.5795	0.5852	0.6023	0.5818
	NGK	0.6136	0.6193	0.6278	0.6420	0.6534	0.6301
	Lasso	0.5795	0.5966	0.6051	0.6080	0.6136	0.6011
Patient A's NR vs. Patient B's NR	Ridge	0.6933	0.7200	0.7267	0.7333	0.7467	0.7253
	NGK	0.6667	0.6800	0.7067	0.7200	0.7200	0.7013
	Lasso	0.7200	0.7333	0.7467	0.7600	0.7867	0.7453
Patient A's CA vs. MDA-MB-231	Ridge	0.6193	0.6307	0.6364	0.6420	0.6534	0.6369
	NGK	0.6477	0.6591	0.6705	0.6818	0.6818	0.6687
	Lasso	0.6420	0.6534	0.6619	0.6705	0.6761	0.6608
Patient A's CA vs. MCF-7	Ridge	0.7403	0.7514	0.7597	0.7735	0.7845	0.7624
	NGK	0.7790	0.7845	0.7928	0.7956	0.8066	0.7923
	Lasso	0.7845	0.7956	0.8066	0.8122	0.8122	0.8033

Patient A's CA vs. HCC1806	Ridge	0.7979	0.8138	0.8138	0.8191	0.8298	0.8144
	NGK	0.8298	0.8404	0.8431	0.8511	0.8617	0.8447
	Lasso	0.8298	0.8351	0.8404	0.8457	0.8511	0.8415
Patient B's CA vs. MDA-MB-231	Ridge	0.6198	0.6302	0.6406	0.6458	0.6562	0.6391
	NGK	0.6615	0.6771	0.6823	0.6875	0.6927	0.6813
	Lasso	0.6927	0.6979	0.7083	0.7083	0.7240	0.7052
Patient B's CA vs. MCF-7	Ridge	0.6802	0.6904	0.6980	0.7056	0.7157	0.6985
	NGK	0.7360	0.7513	0.7589	0.7614	0.7665	0.7558
	Lasso	0.7411	0.7563	0.7614	0.7665	0.7766	0.7604
Patient B's CA vs. HCC-1806	Ridge	0.7451	0.7549	0.7549	0.7647	0.7696	0.7574
	NGK	0.7549	0.7696	0.7745	0.7745	0.7892	0.7730
	Lasso	0.7598	0.7794	0.7843	0.7892	0.7941	0.7828
Patient A's NR vs. MCF-10A	Ridge	0.8828	0.8828	0.8906	0.8906	0.9141	0.8914
	NGK	0.8828	0.8906	0.8906	0.8906	0.8984	0.8898
	Lasso	0.8438	0.8516	0.8594	0.8594	0.8828	0.8586
Patient B's NR vs. MCF-10A	Ridge	0.8516	0.8581	0.8581	0.8645	0.8645	0.8587
	NGK	0.8194	0.8258	0.8323	0.8387	0.8452	0.8323
	Lasso	0.8258	0.8387	0.8452	0.8516	0.8516	0.8432
Patient A & B's CA vs. Patient A& B's NR	Ridge	0.6233	0.6279	0.6419	0.6512	0.6698	0.6423
	NGK	0.6454	0.6574	0.6633	0.6653	0.6733	0.6614
	Lasso	0.6335	0.6574	0.6614	0.6693	0.6813	0.6622